MEDICAL SCIENCE MONITOR

ANIMAL STUDY

e-ISSN 1643-3750
© Med Sci Monit, 2020; 26: e919150
DOI: 10.12659/MSM.919150

Received: 2019.08.03
Accepted: 2019.11.21
Available online: 2020.01.21
Published: 2020.02.13

Effect of Grilled Nux Vomica on Differential RNA Expression Profile of Gastrocnemius Muscle and Toll-Like Receptor 4 (TLR-4)/Nuclear Factor kappa B (NF-κB) Signaling in Experimental Autoimmune Myasthenia Gravis Rats

Authors' Contribution:
Study Design A
Data Collection B
Statistical Analysis C
Data Interpretation D
Manuscript Preparation E
Literature Search F
Funds Collection G

ABCEF 1 Xu Hong Jiang
ACEF 1 Yi Chen
BCF 1 Yang Yang Ding
BCDF 2 Hui Qiu
EFG 3 Di Yi Zhou
ACEFG 4 Chang Lin Qiu

1 Department of Emergency Medicine, First Affiliated Hospital of Zhejiang Chinese Medical University, Hangzhou, Zhejiang, P.R. China
2 Department of Traditional Chinese Medicine (TCM), Third Affiliated Hospital of Zhejiang Chinese Medical University, Hangzhou, Zhejiang, P.R. China
3 Department of Endocrinology, Zhejiang Integrated and Western Medicine Hospital, Hangzhou, Zhejiang, P.R. China
4 Department of Neurology, First Affiliated Hospital of Zhejiang Chinese Medical University, Hangzhou, Zhejiang, P.R. China

Corresponding Author: Chang Lin Qiu, e-mail: qiuclyxzcmu@163.com
Source of support: This work was supported by the Science and Technology Plan of Zhejiang Traditional Chinese Medicine (grant no. 2014ZA048)

Background: Myasthenia gravis (MG) is a progressive autoimmune disorder caused by the production of antibodies directed against acetylcholine receptors (AChRs), resulting in muscle weakness and fatigue. This study aimed to explore the effect and mechanism of grilled nux vomica (GNV) in experimental autoimmune myasthenia gravis (EAMG) rats.

Material/Methods: Rat 97–116 peptides were used to mediate disease in the EAMG model in SPF female Lewis rats. The treatment groups received grilled nux vomica (75 mg/kg, 150 mg/kg, and 225 mg/kg). The autoantibody and inflammatory cytokines levels were measured by enzyme-linked immunosorbent assay (ELISA). RNA profiling was performed on high-dose and model group rats. Profiling results and TLR-4/NF-κB signaling were validated by q-PCR and Western blot analysis.

Results: The results showed that GNV could attenuate the symptoms of EAMG rats. There was a decreased level of AChR-ab, IFN-γ, TNF-α, IL-2, IL-4, and IL-17 levels, and an increased level of TGF-β1. In total, 235 differentially expressed genes (DEGs), consisting of 175 upregulated DEGs and 60 downregulated DEGs, were identified. Functional annotation demonstrated that DEGs were largely associated with leukocyte cell–cell adhesion, NF-kappa B signaling pathway, muscle contraction, and cardiac muscle contraction pathway. Rac2, Itgb2, Lcp2, Myl3, and Tnni1 were considered as hub genes with a higher degree value in the protein–protein interaction (PPI) network. The q-PCR and Western blot results of hub genes were consistent with RNA profiles. GNV treatment also significantly reduced the TLR-4 and NF-κB p65 protein expression in EAMG rats.

Conclusions: These results indicate that grilled nux vomica ameliorates EAMG by depressing the TLR-4/NF-κB signaling pathway, and hub genes may serve as potential targets for MG treatment.

MeSH Keywords: Gene Expression Profiling • Muscle, Skeletal • Myasthenia Gravis, Autoimmune, Experimental

Full-text PDF: https://www.medscimonit.com/abstract/index/idArt/919150

Indexed in: [Current Contents/Clinical Medicine] [SCI Expanded] [ISI Alerting System] [ISI Journals Master List] [Index Medicus/MEDLINE] [EMBASE/Excerpta Medica] [Chemical Abstracts/CAS]

Background

Myasthenia gravis (MG), a T cell-dependent autoimmune disease, is mediated by specific autoantibodies at the neuromuscular junction (NMJ) and results in distinctive fatigability and limb weakness [1,2]. Experimental autoimmune myasthenia gravis (EAMG) is used as a common model of MG, in which female Lewis rats are immunized with AChR R97-116 peptide [3,4]. After immunization, EAMG animals closely mimic the clinical symptoms, anti-acetylcholine receptors (AChR) antibodies, electrophysiological signs, and immunological parameters of human MG, suggesting that the Lewis rat model is suitable for investigating novel therapeutic avenues in MG. MG also is a chronic inflammatory autoimmune disease. It has been traditionally believed that a highly ordered immune system depends on the balance between anti-inflammatory and pro-inflammatory signals [5]. Many studies in recent years have demonstrated that MG patients have significantly increased expression of pro-inflammatory mediators, including IL-6, TNF-α, interferon (IFN)-γ, and IL-1β [5,6]. At present, the main treatments of MG consist of corticosteroids and immunosuppressants, plasma-exchange, and intravenous immunoglobulin for short-term immunomodulation [7]. However, these treatments often have serious adverse effects due to their inhibition of immunity. Therefore, there is an urgent need for more effective agents with fewer adverse effects to treat MG. Thus, we focused on Traditional Chinese Medicine (TCM) and observed the benefits and mechanisms in the treatment of EAMG Lewis rats.

Nux vomica, the seed of *Strychnos nux vomica L*, is characterized in TCM as being bitter and warm in nature and belongs to the liver and spleen meridians based on the theory of TCM. Additionally, brucine and strychnine are identified as the central toxic and principal bioactive compounds, respectively [8]. Studies have suggested that nux vomica strengthens the central nervous systems [8,9] and possesses analgesic, anti-inflammatory [10], and anti-tumor properties [8]. Furthermore, modern experimental research has demonstrated its immunomodulatory effects. Zou et al. reported that GNV decreased acetylcholine receptor antibody (AChR-ab) levels in EAMG rats [11]. These studies demonstrated the possible clinical value of nux vomica in treatment of autoimmune diseases. The exact anti-inflammatory molecular mechanisms of nux vomica are still largely unknown, and many studies suggest that its anti-inflammatory effect is correlated reduced release of pro-inflammatory cytokines in adjuvants-induced arthritis rats [12].

So far, there is no report about the effect of nux vomica on inflammation under EAMG. In this research, we hypothesized that GNV has a therapeutic effect on EAMG, and aimed to preliminarily assess the potential therapeutic targets and underlying mechanism of GNV capsules on the pathogenesis of EAMG by use of RNA expression profiling.

Material and Methods

Animals

Sixty Lewis rats (6 weeks old, 120–138 g) were used in this study. The rats were obtained from Beijing Vital River Laboratories (Beijing, China; license number: SCXK (Beijing) 2012-0001). All rats were housed in the Animal Center of Zhejiang Chinese Medicine University with a 12-h light/12-h dark cycle, and had free access to standard rat chow and water. All animal experiments were approved by the Animal Care and Welfare Committee of Zhejiang Chinese Medical University (permit number: ZSLL-2019-92, Zhejiang, China). Animal suffering was kept to a minimum, and tissues were harvested after euthanasia by chloral hydrate (TCI Chemical Industrial Development Co., Shanghai, China).

Induction of EAMG and clinical evaluation

The EAMG model was prepared based on previously described methods [13]. We subcutaneously injected 52 rats with 100 μg/200 μL Rat 97-116 peptides (DGDFAIVKFTKVLLDYTGHI, CL Bio-Science Co., Xian, China) in Complete Freund's adjuvant (CFA, Sigma) in the waist, abdomen and hind-foot pads, and boosted with 50 μg Rat 97–116 peptides in 200 μl of incomplete Freund's adjuvant (IFA, Sigma) on days 30 and 45, respectively. The control rats were injected with CFA emulsified in PBS and boosted with IFA in PBS at the same sites. According to the EAMG clinical scale score in a rat model proposed by Lennon et al. [14], clinical evaluation was scored as follows: 0, no fatigue and normal strength; 1, slightly impaired activity, fatigable, and weak grip; 2, weakness, tremor, head down, hunched posture presented before clinical signs; 3, severe weakness, no grip moribund; and 4, death. We used 0.5 increments as intermediate scores assigned to rats with intermediate signs. Lennon scores are presented as the average value of each group at modeling time point.

Nux vomica preparation and animal treatment

Nux vomica (lot no. 170518) was prepared by removing extraneous material, soaking, stir-frying, drying, powdering, and disinfecting at Zhejiang Provincial Hospital of TCM, and each capsule contained 0.2 g of grilled nux vomica. The 40 EAMG rats were split into 5 groups (n=8): a model group, a low-dose group, a middle-dose group, a high-dose group, and a prednisone group (the positive group). EAMG rats received intragastric administration of 75 mg/kg (low-dose group), 150 mg/kg (middle-dose group), and 225 mg/kg (high-dose group) GNV and 4 mg/kg prednisone dissolved in 0.2% sodium carboxymethylcellulose (CMC-Na) solution once a day for 4 weeks. The control and model groups (n=8) received the same volume of CMC-Na solution. After the last immunization and treatment,

Indexed in: [Current Contents/Clinical Medicine] [SCI Expanded] [ISI Alerting System] [ISI Journals Master List] [Index Medicus/MEDLINE] [EMBASE/Excerpta Medica] [Chemical Abstracts/CAS]

the parameters of holding power and Lennon scores were recorded. Animal weights were measured every week during treatment.

Repetitive nerve stimulation (RNS) test

All animals were fixed on the BL-420S system under anesthesia with 10% chloral hydrate (intraperitoneal). Then, a stimulating electrode was inserted into the gastrocnemius muscle near the sciatic nerve. Subsequently, a reference electrode was inserted into abdominal subcutaneous tissue. In addition, 2 recording electrodes were inserted into the subcutaneous tissue. All the electrodes received a 5 Hz electrical stimulus 10 times. The attenuation value of RNS (D)=(first responses minus the fifth responses)/first responses×100%.

ELISA

After treatment, heart blood was rapidly collected from sacrificed rats, then the blood centrifuged at 3000 rpm for 20 min at 4°C to prepare serum samples. Concentrations of serum AChR-ab, IFN-γ, TNF-α, IL-2, IL-4, IL-17, and TGF-β1 in individual rats were detected by ELISA kit (Nanjing SenBeiJia Bio-Technology Co., Nanjing, China) according to the manufacturer's instructions.

RNA sequencing

The gastrocnemius muscle was harvested from rats in the model and high-dose groups for subsequent array analysis. The RNA sequencing was conducted at LC-Bio Co. (Hangzhou, China). In brief, total RNA of gastrocnemius muscle tissue specimens was extracted with Trizol solution (Invitrogen, CA, USA) based on the manufacturer's operating instructions. The purity and quantity of total RNA were estimated using the Bioanalyzer device (Agilent, USA) with the RNA integrity number >7.0. Poly(A) RNA was purified from the total RNA (5 μg) using poly-T oligo-attached magnetic beads with 2 rounds of purification. After purification, the messenger RNA was cut into small pieces with divalent cations at increasing temperatures. The complementary DNA (cDNA) library was subsequently constructed using reverse transcription with the cleaved fragments of RNA according to the protocol of the RNA-Seq sample preparation kit (Illumina, San Diego, USA), and the average insert size for the paired-end libraries was 300±50 bp. Then, we conducted the sequencing on an IlluminaHiseq4000 platform (LC Sciences, USA).

RNA sequencing data and bioinformatics analysis

We aligned reads of the model and high-dose group samples to the UCSC (*http://genome.ucsc.edu/*) [15] rats' reference genome by using the R package of HISAT. The mapped reads of each sample were assembled using StringTie. Then, all transcriptomes from gastrocnemius muscle samples were integrated to reconstruct a complete transcriptome using Perl scripts. Finally, StringTie and edgeR were employed to estimate the expression levels of all transcripts. The DEGs were identified with $\log_2$ (Fold change, FC) >1 or log2 (FC) <–1 with significant difference (p value <0.05) by R package. The data were visualized with a hierarchical cluster analysis by using GeneSpring (version 7.2) software (Silicon Genetics, CA). The annotation of upregulated/downregulated DEGs was done according to the Metascape database (*http://metascape.org/*) [16], a gene annotation and analysis resource. Furthermore, the STRING database (*http://string-db.org/*) [17] was used to construct the protein–protein interaction (PPI) networks of up-/downregulated DEGs with combined score >0.4 as the cut-off criterion, and then visualized with Cytoscape (Version 3.6.1; *http://cytoscape.org/*) software. The DEGs act as nodes in the PPI network, and the degree value represents the number of interacting proteins. A node with a higher degree is considered to be the hub node. By analyzing the degree value of the nodes in the PPI up-/downregulated networks, respectively, the hub genes were acquired.

Quantitative real-time PCR

Total RNA was extracted from the same gastrocnemius muscle samples as in the microarray research, using Trizol reagent (Sigma, St. Louis, MO, USA) according to the manufacturer's protocol. The extracted RNA was reverse-transcribed to cDNA with the PrimeScript RT Master Mix (TaKaRa). Then, the real-time PCR was conducted using a TaqMan Universal Master Mix II kit on an Applied Biosystems 7500 Sequence Detection System (Applied Biosystem). The primers for Rac family small GTPase 2 (Rac2), integrin subunit beta 2 (Itgb2), lymphocyte cytosolic protein 2 (Lcp2), myosin light chain 3 (Myl3), and troponin I1, slow skeletal type (Tnni1) are as shown in Table 1. Glyceraldehyde-3-phosphate dehydrogenase (GAPDH) was selected as the internal standard control. The relative mRNA expression levels for hub genes were determined by using the Ct ($2^{-\Delta\Delta Ct}$) method.

Western blot assay

The gastrocnemius muscle tissues were lysed using ice-cold RIPA lysis buffer (Beyotime Biotech, Shanghai, China) supplemented with 1% phenylmethylsulfonyl fluoride (PMSF), and then centrifuged at 12 000 rpm for 15 min at 4°C. Then, the protein concentration was quantified using a bicinchoninic acid (BCA) protein assay kit (Thermo Scientific, USA). We used primary antibodies against Rac2 (#ab154711, 1: 2000; Abcam, Cambridge, MA), Itgb2 (#73663, 1: 1000; Cell Signaling), Lcp2 (#4958, 1: 1000; Cell Signaling), Myl3 (#ab680, 1: 100; Abcam, Cambridge, MA), Tnni1 (#ab231720, 1: 2000; Abcam,

Indexed in: [Current Contents/Clinical Medicine] [SCI Expanded] [ISI Alerting System] [ISI Journals Master List] [Index Medicus/MEDLINE] [EMBASE/Excerpta Medica] [Chemical Abstracts/CAS]

Table 1. The primers for RT-PCR.

Gene	Forward primer (5'-3')	Reverse primer (5'-3')
Rac2	TACACCACCAATGCCTTCCC	GTGATGGGAGCCAGCTTCTT
Itgb2	GTTTCAGACAGAGGTCGGCA	TGCTCCTGGATACACTCCGA
Lcp2	ATGGCGCTCGGTTTTTGAAC	CAGGATATCGTGGAACCGGG
Myl3	AATCCTACCCAGGCAGAGGT	TTGCCCTCCTTGTCGAAGAC
Tnni1	AGGCTGAGAAGGTGCGTTAC	GGAGCTCTCGGCATAAGTCC
TLR-4	TGTATCGGTGGTCAGTGTGC	TCCCACTCGAGGTAGGTGTT
NF-κB	GGATAGCACTGGCAGCTTCA	TCCTCCGAAGCTGGACAAAC
GADPH	GCGGGAGCGGATCCTAATA	TGGTGCATCCATGGGCTAC

Rac2– Rac family small GTPase 2; Itgb2 – integrin subunit beta 2; Lcp2– lymphocyte cytosolic protein 2; Myl3– myosin light chain 3; Tnni1– troponin I1, slow skeletal type.

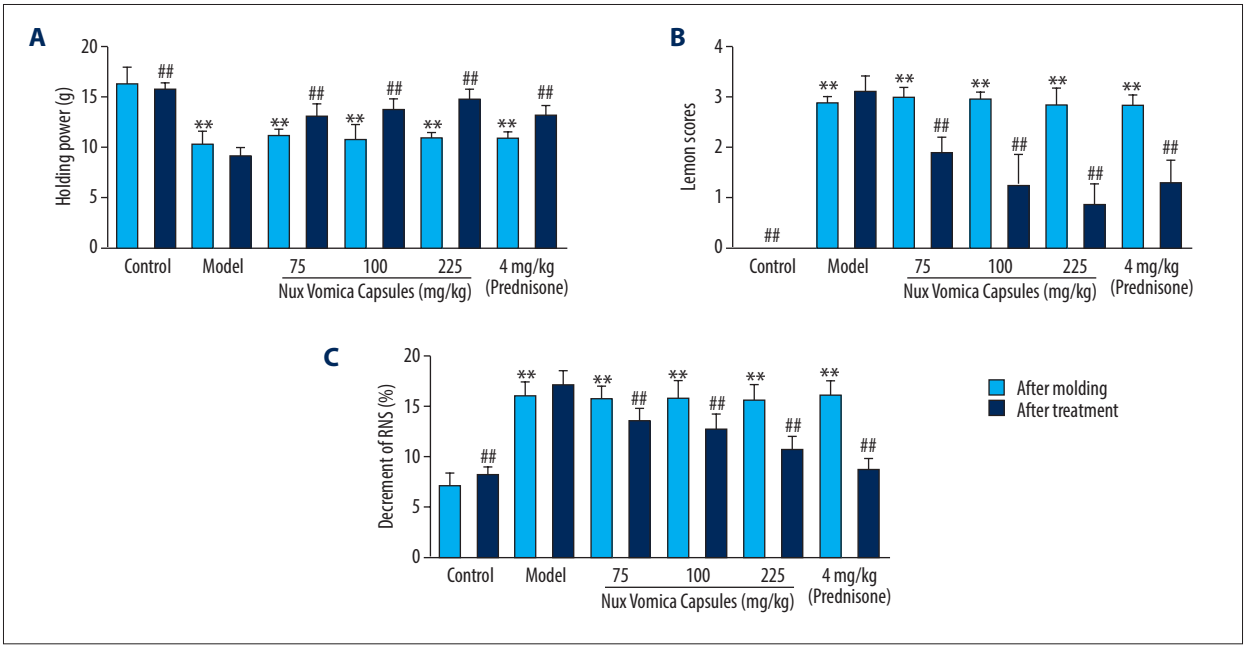

Figure 1. Grilled nux vomica treatment ameliorated the severity of R97-116-induced EAMG in Lewis rats. The holding power (**A**), clinical score (**B**), and decrease in of RNS (**C**) of rats in control and grilled nux vomica-treated groups (n=12 rats/group) were assessed between the after modeling and after grilled nux vomica treatment. Data are expressed as the mean±SD (** $P<0.01$, versus control group; ## $P<0.01$, versus model group). RNS – repetitive nerve stimulation.

Cambridge, MA), Toll-like receptor 4 (TLR-4, #14358, 1: 1000; Cell Signaling), and NF-κB p65 (#8242, 1: 1000; Cell Signaling), followed by incubating with the secondary antibody against IgG (#ab7090 or #ab205719, 1: 5000, Abcam, Cambridge, USA). Protein levels were normalized by probing the same blots with a GAPDH antibody (#3683, 1: 1,000; Cell Signaling). Finally, the protein bands were visualized with an Odyssey® IR scanner (LI-COR, USA) and quantified by Image J (version 1.8.0) software (National Institutes of Health, NY).

Statistical analysis

All data are presented as mean±SD. Data on statistical comparisons between the 2 groups were evaluated with *t* test. P value <0.05 was defined as a statistically significant difference. SPSS v21.0 (IBM Corp, USA) and GraphPad Prism v5.0 software (San Diego, California, USA) were used for statistical analyses.

Indexed in: [Current Contents/Clinical Medicine] [SCI Expanded] [ISI Alerting System] [ISI Journals Master List] [Index Medicus/MEDLINE] [EMBASE/Excerpta Medica] [Chemical Abstracts/CAS]

Table 2. Comparison of average weight among the groups after grilled nux vomica treatment.

Groups	Average weight (after nux vomica treatment) (g)				n
	1st week	2th week	3rd week	4th week	
Control	226.8±4.2	237.7±4.6**	247.5±7.0**	266.1±6.8**	8
Model	187.3±2.5##	182.2±4.0	174.2±4.4	157.4±5.9	8
Low-dose group	188.0±4.5##	197.8±6.3**	202.1±8.1**	216.4±6.4**	8
Middle-dose group	188.4±8.2##	200.9±5.5**	217.6±5.7**	233.3±5.4**	8
High-dose group	190.9±6.4##	212.9±4.3**	225.0±3.7**	244.4±5.7**	8
Prednisone group	185.7±2.9##	191.2±5.2**	220.4±8.4**	249.3±11.1**	8

The results are expressed as mean±SD (n=8 rats/group). Comparison of average weight in the control, model, low-, middle-, and high-dose groups after grilled nux vomica treatment, respectively, ## P<0.01; The model, high-, middle- and low-dose groups *vs.* control group; ** P<0.01; The control, high-, middle- and, low-dose groups *vs.* model group.

Results

GNV capsules ameliorate EAMG symptoms

After modeling, the weakness symptoms of EAMG Lewis rats became more obvious, including a humped back, an obvious tremor, and significantly decreased activity. There were statistically significant differences in holding power (Figure 1A, P<0.01) and Lennon scores (Figure 1B, P<0.01) and a decrease in RNS (Figure 1C, P<0.01) when compared to the control group before GNV capsules treatment. Statistical analysis suggested that GNV at 75 mg/kg/day, 150 mg/kg/day, and 225 mg/kg/day decreased the holding power and decreased the clinical Lennon scores for RNS of the treatment groups compared with the model group. Additionally, the effect of GNV on the average body weight was examined weekly during therapy. The average body weight of the model group observably decreased after administration of normal CMC-Na (P<0.01, Table 2). GNV and prednisone both reduced the severity of EAMG, and the average body weights of the treatment groups were significantly higher than in the model group (P<0.01). The results showed that GNV has a therapeutic effect on EAMG.

Detection of AChR-ab, TGF-β1, and inflammatory mediators in EAMG

It has been reported that AChR-ab, TGF-β1, and inflammatory mediators are closely related to the process of EAMG; therefore, we used ELISA to estimate the level of AChR-ab, IFN-γ, IL-4, IL-17, TNF-α, IL-2, and TGF-β1 in serum samples. As shown in Figure 2A–2D, the low-dose, middle-dose, and high-dose GNV groups lower levels of AChR-ab, IFN-γ, IL-4, and IL-17 in EAMG rats in comparison with the model group (P<0.01). Similarly, the levels of TNF-α and IL-2 were lower in the middle-dose and high-dose groups than in the model group (Figure 2E, 2F; P<0.01), and there was no significant difference between the low-dose and the model group. Additionally, the TGF-β1 level was clearly higher in the treated groups than in the model group (Figure 2G, P<0.01).

Identification of DEGs and functional enrichment analysis

We used the gastrocnemius muscle samples of GNV-treated EAMG rats compared with healthy tissues to select EAMG-associated genes. According to the criteria of P<0.05 and |logFC| >1, 235 DEGs were identified, including 175 upregulated DEGs and 60 downregulated DEGs. Notably, the proportion of upregulated genes was larger than that of downregulated genes in treated groups compared to the model group. The distribution of the 2 groups of DEGs at the logFC and P value levels is shown in Figure 3A. A heat map of hierarchical clustering analysis for the DEGs is shown in Figure 3B, which was created based on the gene expression level and, the results demonstrated a clearly different expression pattern.

To further understand the functional classification of the specific genes, we used the Metascape platform to investigate the biological processes (BP) and the Kyoto Encyclopedia of Genes and Genomes (KEGG) pathways of DEGs. The result of GO analysis demonstrated that the upregulated DEGs were most observably enriched in the leukocyte cell–cell adhesion, immune effector, and regulation of the immune response process (Figure 3C). KEGG analysis indicated that the upregulated DEGs were enriched in NF-kappa B signaling pathway and phospholipase D signaling pathway, as well as the disease-related pathway, which include *Staphylococcus aureus* infection, tuberculosis, type I diabetes mellitus, and autoimmune thyroid disease (Figure 3D). Similarly, the downregulated DEGs were mainly enriched in BP terms of muscle contraction and structure development process (Figure 3E). The downregulated DEGs were mainly involved in hypertrophic cardiomyopathy, cardiac muscle contraction, dilated cardiomyopathy, and thyroid hormone signaling pathway (Figure 3F).

Indexed in: [Current Contents/Clinical Medicine] [SCI Expanded] [ISI Alerting System] [ISI Journals Master List] [Index Medicus/MEDLINE] [EMBASE/Excerpta Medica] [Chemical Abstracts/CAS]

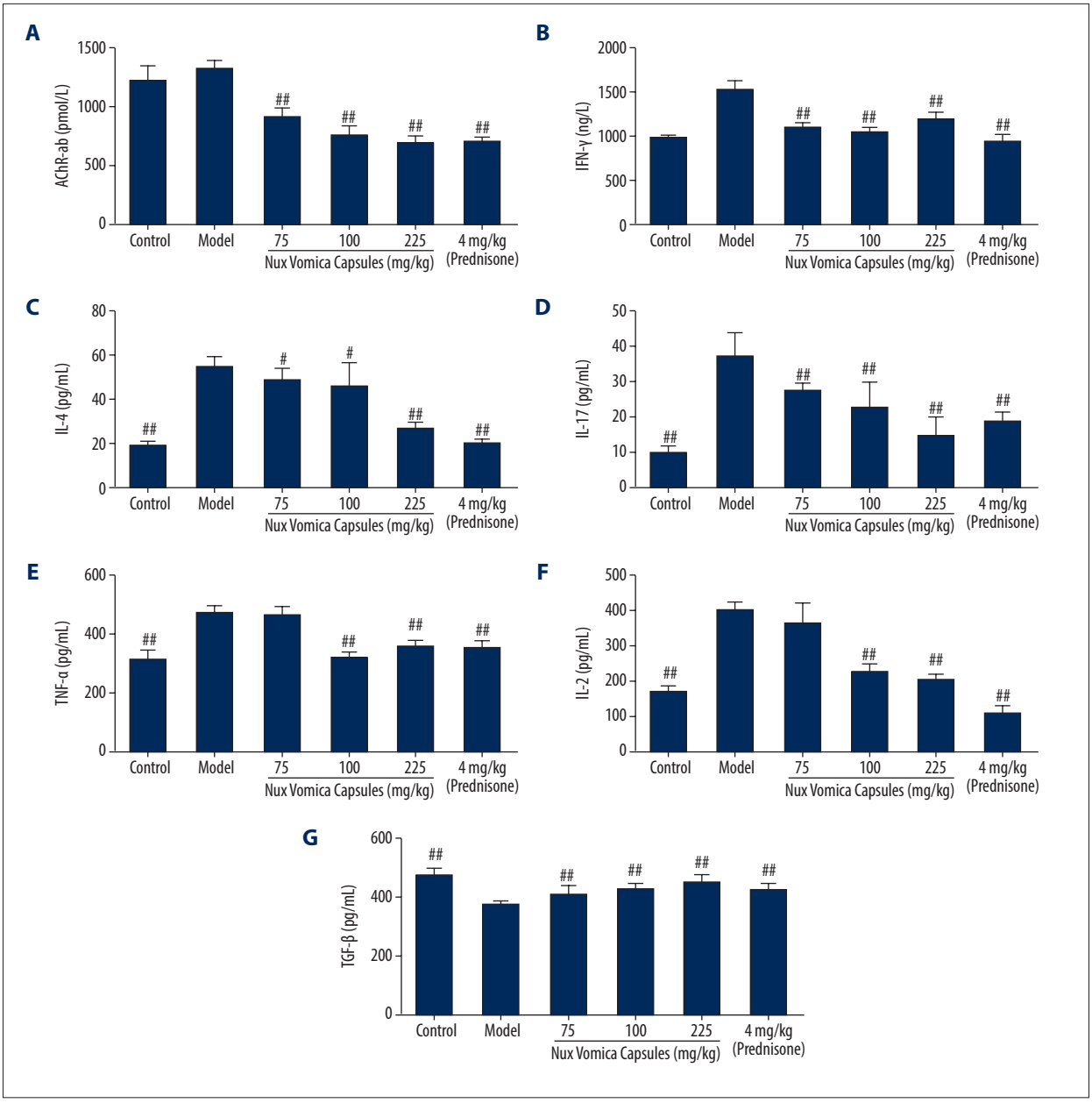

Figure 2. Grilled nux vomica regulates biochemical parameters of serum in EAMG rats. The levels of AChR-ab (**A**), IFN-γ (**B**), IL-4 (**C**), IL-17 (**D**), TNF-α (**E**), IL-2 (**F**), and TGF-β (**G**) in serum analyzed by ELISA. The results are expressed as mean±SD (n=12 rats/group), and $^{\#}$ $P<0.05$; $^{\#\#}$ $P<0.01$, versus model group.

PPI network construction and analysis

Up-/downregulated DEGs were analyzed by STRING and visualized with Cytoscape, respectively. Ultimately, the PPI network of upregulated DEGs was established with 135 nodes and 746 edges. The proteins Rac2 (degree=53), Itgb2 (degree=46), and Lcp2 (degree=40) were used as hub nodes in the upregulated network (Figure 4A). The PPI network for downregulated DEGs, as shown in Figure 4B, had 23 nodes and 78 edges. The top 2 hub proteins – Myl3 (degree=16) and Tnni1 (degree=15) – were selected as hub nodes in this network.

RNA profile validation

We performed q-PCR and Western blot analyses to validate the results of RNA profiling. Three upregulated DEGs (Rac2, Itgb2, Lcp2) and 2 downregulated DEGs (Myl3 and Tnni1) were confirmed to be altered across all 4 gastrocnemius muscles samples. The q-PCR and Western blotting results indicated that the

Indexed in: [Current Contents/Clinical Medicine] [SCI Expanded] [ISI Alerting System] [ISI Journals Master List] [Index Medicus/MEDLINE] [EMBASE/Excerpta Medica] [Chemical Abstracts/CAS]

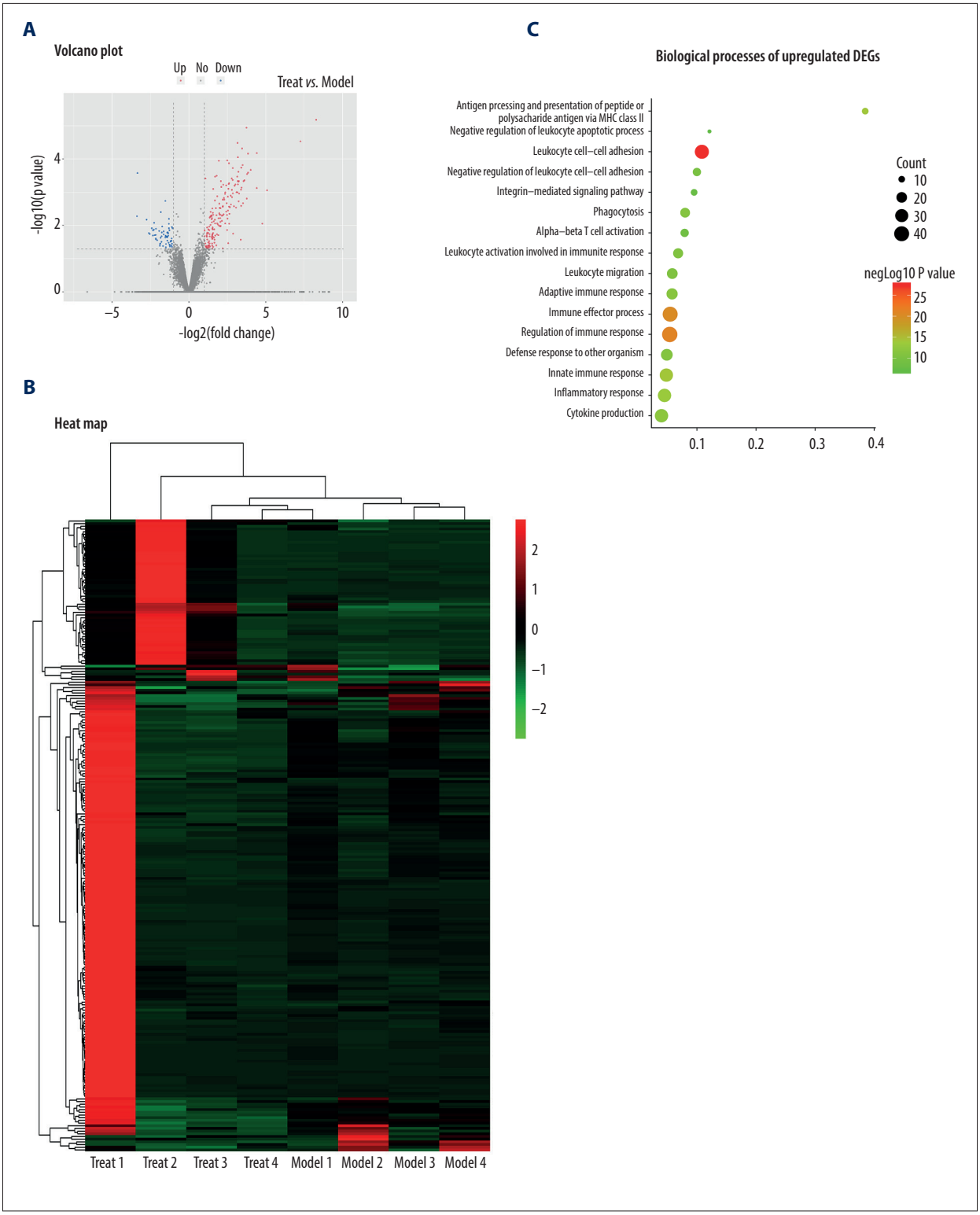
A
Volcano plot
Up No Down
Treat vs. Model
-log10(p value)
-log2(fold change)
B
Heat map
Treat 1
Treat 2
Treat 3
Treat 4
Model 1
Model 2
Model 3
Model 4
C
Biological processes of upregulated DEGs
Antigen prcessing and presentation of peptide or polysacharide antigen via MHC class II
Negative regulation of leukocyte apoptotic process
Leukocyte cell–cell adhesion
Negative regulation of leukocyte cell–cell adhesion
Integrin–mediated signaling pathway
Phagocytosis
Alpha–beta T cell activation
Leukocyte activation involved in immunite response
Leukocyte migration
Adaptive immune response
Immune effector process
Regulation of immune response
Defense response to other organism
Innate immune response
Inflammatory response
Cytokine production
Count
negLog10 P value

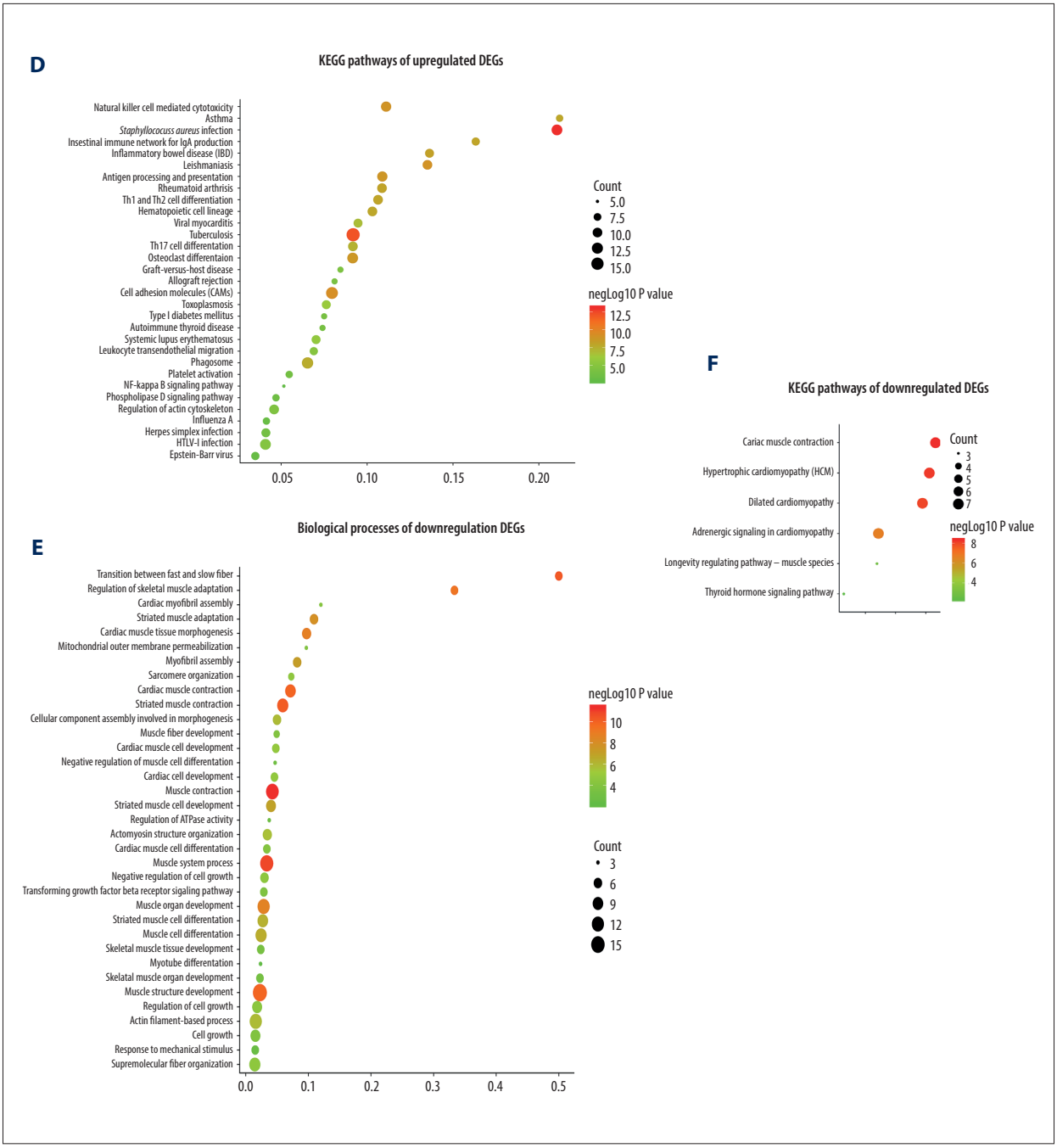

Figure 3. Identification of DEGs between grilled nux vomica-treated group (225 mg/kg) and model group, and bioinformatics analysis of up-/downregulated DEGs. (**A**) Volcano plots of DEGs. There were 175 genes upregulated and 60 downregulated genes in gastrocnemius muscle. Hierarchical clusters of the DEGs in the treated groups and model group (**B**). Biological processes (**C**) and KEGG pathways enrichment analyses (**D**) of upregulated DEGs. Biological processes (**E**) and KEGG pathways enrichment analyses (**F**) of downregulated DEGs. DEGs – differently expressed genes.

Indexed in: [Current Contents/Clinical Medicine] [SCI Expanded] [ISI Alerting System] [ISI Journals Master List] [Index Medicus/MEDLINE] [EMBASE/Excerpta Medica] [Chemical Abstracts/CAS]

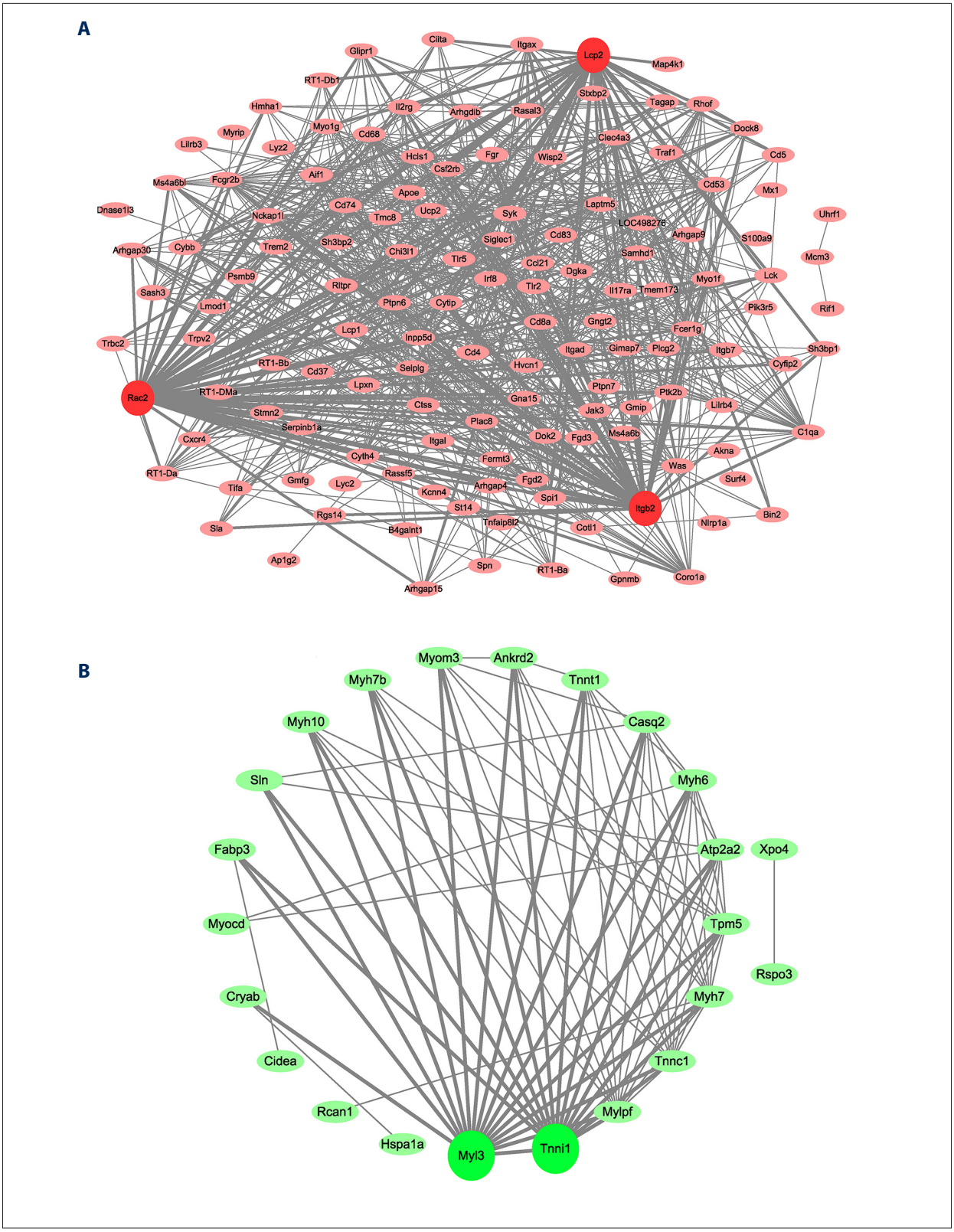

Figure 4. Protein–protein interaction (PPI) network for the DEGs. PPI network of upregulated DEGs (**A**). PPI network of downregulated DEGs (**B**). Red nodes, upregulated genes; green nodes, downregulated genes; (Rac2, Lcp2, and Itgb2) as well as (Myl3 and Tnni1) are the hub genes in upregulated and downregulated network with a higher degree value.

Indexed in: [Current Contents/Clinical Medicine] [SCI Expanded] [ISI Alerting System] [ISI Journals Master List] [Index Medicus/MEDLINE] [EMBASE/Excerpta Medica] [Chemical Abstracts/CAS]

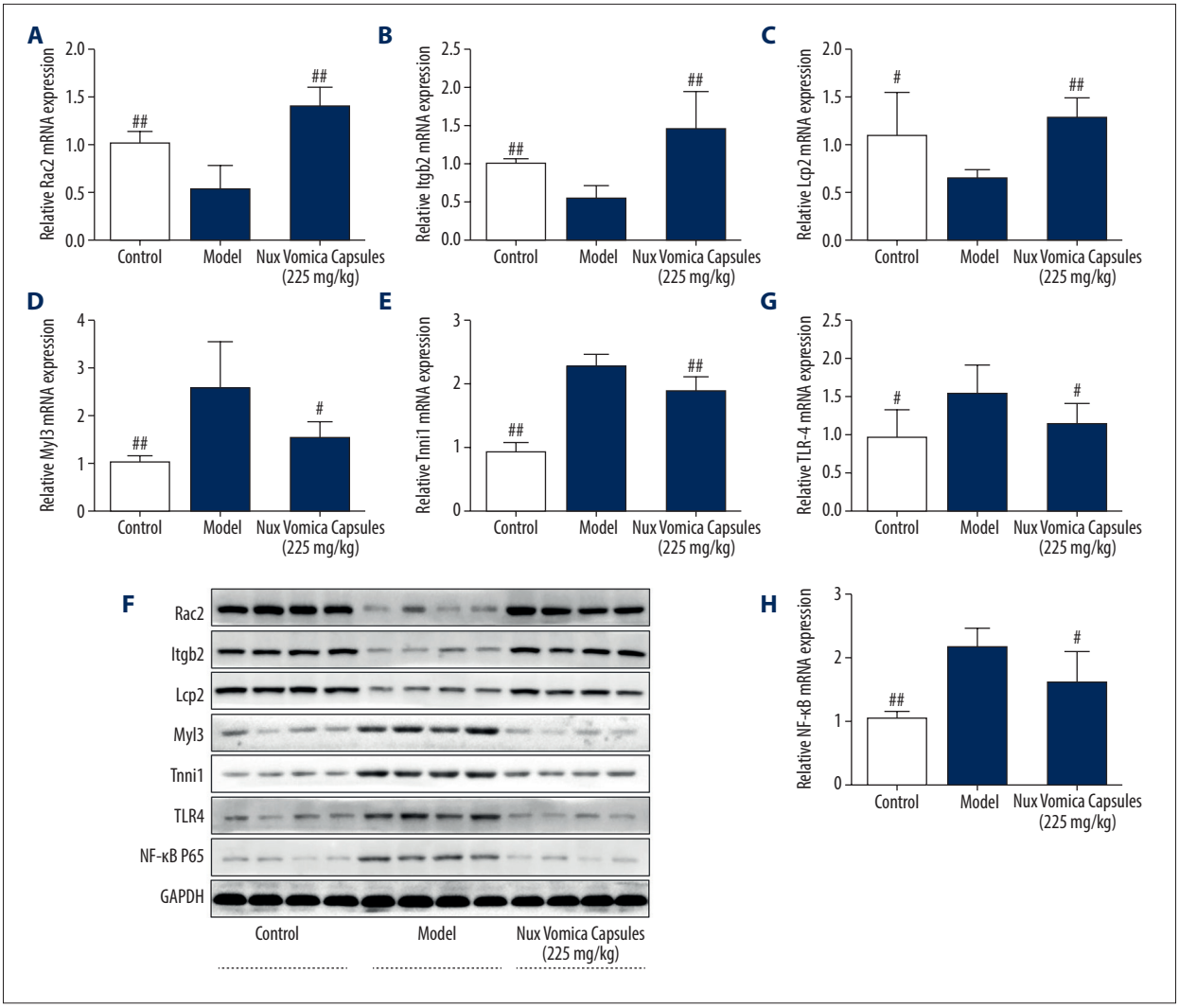

Figure 5. Grilled Nux Vomica regulates hub genes and the TLR-4/NF-κB pathway in the gastrocnemius muscle of EAMG rats. The mRNA expression level of Rac2 (**A**), Itgb2 (**B**), Lcp2 (**C**), Myl3 (**D**), and Tnni1 (**E**) was measured by quantitative real-time PCR (q-PCR). Additionally, the protein expression level of Rac2, Itgb2, Lcp2, Myl3, Tnni1, TLR-4, and NF-κB p65 (**F**) was determined by Western blot. Further, the transcriptional expression level of TLR-4 (**G**) and NF-κB (**H**) was assessed with q-PCR. Data are presented as mean±SD, and $^{\#}$ $P<0.05$; $^{\#\#}$ $P<0.01$, versus model group.

mRNA and protein expressions of Rac2, Itgb2, and Lcp2 were significantly higher in the GNV (225 mg/kg)-treated samples compared with that in the model samples (Figure 5A–5C), while the mRNA and protein levels of Myl3 and Tnni1 were lower in GNV-treated samples than in the model samples (Figure 5D–5F). These results were similar to the results acquired using microarray analysis, suggesting that the hub genes from the mRNA microarray analysis were reliable and could be used for further analysis of potential mechanisms.

Effect of GNV on EAMG of TLR-4/NF-κB signaling

Compared with the control group, the model group had higher TLR-4 and NF-κB mRNA and protein levels. GNV treatment improved EAMG rats, as shown by downregulated TLR-4 and NF-κB p65 levels (Figure 5F–5H). These results suggest that GNV treatment observably inhibited TLR-4/NF-κB pathway activity in EAMG rats.

Discussion

The EAMG model of a chronic autoimmune disease was induced with a synthetic rat 97~116 peptide. First-line therapies for neurological autoimmune diseases depend on generalized immunosuppression, which is often associated with adverse effects. Therefore, the search for new and better therapies may help to enhance quality of life of MG patients. In the

Indexed in: [Current Contents/Clinical Medicine] [SCI Expanded] [ISI Alerting System] [ISI Journals Master List] [Index Medicus/MEDLINE] [EMBASE/Excerpta Medica] [Chemical Abstracts/CAS]

present study, we discovered that treatment with GVN capsules improved the holding power and depressed the Lennon scores of EAMG female Lewis rats. Further, we found that GVN treatment ameliorated the decreased RNS in EAMG rats. This study provides convincing evidence that GVN is effective in depressing the severity of disease and symptoms in EAMG rats.

Muscle weakness is mostly caused by autoantibodies specific to AChR at the NMJ in the EAMG rat model [18,19]. Hence, depressing anti-AChR IgG secretion could be a promising therapeutic strategy for EAMG. Using the aforementioned therapeutic method, we assessed whether GVN could affect anti-AChR antibody secretion *in vivo*. Results of ELISA in serum suggested that GVN-treated EAMG rats produced significantly reduced levels of AChR-ab, and the effect was dose-dependent. *In vivo* findings indicated that treatment with GVN modulated the initiation and progression of EAMG. Further, the secretion of inflammatory cytokines and imbalance of Th1/Th17/Th2/Treg immune cells play a central role in the pathogenesis of EAMG. Th1 responses are essential in the pathogenesis of EAMG and are correlated with IFN-γ and TNF-α [20,21]. Also, Th17 cells play a significant role in predisposing to EAMG by secreting IL-17 [20,22]. TGF-β1, an important endogenous immunoregulator, is expressed in mammals and is involved in many pathophysiological activities. TGF-β1 suppresses B cell proliferation and downregulates IFN-γ production, suggesting an important role of TGF-β1 of EAMG [23]. Our results showed that GVN decreased the levels of IFN-γ, TNF-α, IL-2, IL-4, and IL-17 and increased TGF-β1 levels, indicating that GVN regulates the imbalance between Th1/Th2/Th17 cells in EAMG to limit disease progression.

A different biological effect of neuromuscular disorders on particular muscle groups was found in numerous clinical observations. Our present RNA microarray analysis of the gastrocnemius muscle with GVN treatment showed that 175 upregulated genes were significantly associated with leukocyte cell–cell adhesion and NF-kappa B signaling pathway, and 60 downregulated genes were related to muscle contraction. This finding suggests that the abnormalities of the immune system and inflammation are significant causes of the progression of MG.

To further screen out the hub genes from these up-/downregulated DEGs, we screened them through network topology calculation of PPI networks. We found 5 genes with higher degree values – Rac2, Itgb2, Lcp2, Myl3, and Tnni1 – in which the changes were consistent with the results of microarray analysis. Rac is a small monomeric GTPase, and possesses 3 different isoforms: Rac1, Rac2, and Rac3 [24]. Rac2, a homolog of Rac1 GTPase, interacts with effector proteins and mediates multiple biological events when combined with GTP [25]; it also is the key signal transducer in inflammatory cells and influences expression of numerous cytokines and growth factors [26]. Ceneri et al. demonstrated that Rac2 deletion results in a basal elevation of inactivated Rac1, and then Rac1 contributes to activation of NF-κB signaling [27]. However, other studies have shown that Rac2 deficiency suppresses pro-inflammatory cytokines and chemokines, as well as fibrosis-related signals in CCl4-induced acute liver injury [28]. Bruder et al. found that atorvastatin reduces the pro-inflammatory actions of aldosterone in vascular smooth muscle cells by inhibiting Rac1/2 [29]. Furthermore, RAC2 may act as a promising prognostic and diagnostic biomarker of clear cell renal cell carcinoma [30], osteosarcoma [31], and prostate cancer [32]. The Itgb2 gene includes 16 exons, coding for the integrin subunit β2 [33], and participates in leukocyte adhesion, activation, and transmigration to sites of inflammation [34]. The present study shows that by increasing expression of Itgb2 in the gastrocnemius muscle, adhesion and trans-endothelial migration of leukocytes is facilitated by grilled nux vomica treatment. Research suggests that the downregulation of lncRNA Itgb2-AS1 inhibits the proliferation, metastasis, and invasion of osteosarcoma [35] and breast cancer [36]. The adaptor protein SLP-76 (also known as Lcp2) is tyrosine phosphorylated by ZAP-70 and is the essential hub for recruitment of SH2 domain-containing signaling proteins [37]. Li et al. reported that Lcp2 plays a significant role in promoting T cell proliferation [38]. Additionally, a splice variant of Lcp2 leads to severe immune dysregulation [39]. Skeletal muscles of rats consist of 2 types – slow-twitch (type I fiber), and fast-twitch (type II) fiber – and Myl3 is an essential myosin light chain 3 of cardiac muscle and is expressed highly in type I skeletal muscle fibers [40]. Maliver et al. demonstrated that significant increases of Myl3 were correlated with myofiber degeneration [41]. TNNI1 is located at 1q31.3, belongs to the TnI subfamily, and encodes the slow skeletal muscle isoform of TnI (ssTnI) [42], which is expressed in the skeletal muscle and heart of embryos [43]. Moreover, ssTnI has been reported to be a sensitive and fast fiber-specific serum marker of skeletal muscle injury [44]. Among these, the Rac2-mediated inflammation, the leukocytes adhesion regulation of Itgb2, the Lcp2-modulated immune process, and the slow-fiber-related genes (Myl3, TNNI1), may play vital roles in the effect of GVN treatment on MG progression.

Additionally, to confirm whether the effects of GVN on the inhibition of inflammation were regulated through inactivation of the TLR-4/NF-κB pathway, the TLR-4 and NF-κB p65 protein expression levels were measured by Western blot. TLR-4, an important transmembrane protein that participates in signal transduction, belongs to the TLR family, and NF-κB is the downstream signaling molecule of TLR-4. Cordiglieri et al. demonstrated that TLR-4 is over-expressed in MG thymuses, and contributed to abnormal cell recruitment in MG thymus via CCL17 and CCL22 [45]. Previous studies have also demonstrated that activated NF-κB protein is transferred into the nucleus to increase pro-inflammatory cytokines TNF-α, IL-6, and IL-1 transcription expression [46]. These results indicate that

Indexed in: [Current Contents/Clinical Medicine] [SCI Expanded] [ISI Alerting System] [ISI Journals Master List] [Index Medicus/MEDLINE] [EMBASE/Excerpta Medica] [Chemical Abstracts/CAS]

the TLR4 and NF-κB p65 protein levels were significantly upregulated in EAMG rats, and these effects were reversed by treatment with GVN. In agreement with KEGG pathways enrichment analysis, our data also show that GVN significantly inhibits TLR-4/NF-κB signaling, which contributes to its anti-inflammatory activity in MG.

Conclusions

In summary, we demonstrated that treatment with grilled nux vomica attenuated the severity of disease in EAMG rats by decreasing the production of pro-inflammatory cytokines and inhibition of TLR-4/NF-κB signaling. These findings indicate that grilled nux vomica, as well as Rac2, Itgb2, Lcp2, Myl3, and Tnni1, have potential as new treatment strategies for MG.

Availability of data and materials

The analyzed datasets generated by our study are available from the corresponding author on reasonable request.

Conflicts of interest

None.

References:

1. Zhang P, Liu RT, Du T et al: Exosomes derived from statin-modified bone marrow dendritic cells increase thymus-derived natural regulatory T cells in experimental autoimmune myasthenia gravis. J Neuroinflammation, 2019; 16(1): 202
2. Jingwei S, Xiaowen L, Wei J et al: Effect of Qiangji Jianli decoction on mitochondrial respiratory chain activity and expression of mitochondrial fusion and fission proteins in myasthenia gravis rats. Sci Rep, 2018; 8(1): 8623
3. Li Z, Li M, Wood K et al: Engineered agrin attenuates the severity of experimental autoimmune myasthenia gravis. Muscle Nerve, 2018; 57(5): 814–20
4. Cui Y, Chang L, Wang C et al: Metformin attenuates autoimmune disease of the neuromotor system in animal models of myasthenia gravis. Int Immunopharmacol, 2019; 75: 105822
5. Villegas JA, Van Wassenhove J, Le Panse R et al: An imbalance between regulatory T cells and T helper 17 cells in acetylcholine receptor-positive myasthenia gravis patients: T reg and T H 17 cells in myasthenia gravis. Ann NY Acad Sci, 2018; 1413(1): 154–62
6. Gradolatto A, Nazzal D, Foti M et al: Defects of immunoregulatory mechanisms in myasthenia gravis: Role of IL-17. Ann NY Acad Sci, 2012; 1274: 40–47
7. Díaz-Manera J, Rojas García R, Illa I: Treatment strategies for myasthenia gravis: An update. Expert Opin Pharmacother, 2012; 13(13): 1873–83
8. Guo R, Wang T, Zhou G et al: Botany, phytochemistry, pharmacology and toxicity of Strychnos nux-vomica L.: A review. Am J Chin Med, 2018: 46(1): 1–23
9. McIntosh RA: Nux vomica and its uses. Can J Comp Med, 1940; 4: 125–27
10. Eldahshan OA, Abdel-Daim MM: Phytochemical study, cytotoxic, analgesic, antipyretic and anti-inflammatory activities of Strychnos nux-vomica. Cytotechnology, 2015; 67(5): 831–44
11. Zou Y, Qiu T, Yang F: Research on the immune regulation mechanism of grilled Nux vomica in experimental autoimmune myasthenia gravis rats. China J Tradit Chin Med Pharm, 2015; 30: 2994–98
12. Qin JH: The intervention of *Semen stychni* on the inflammatory factors in the serum of AA rats. China Pract Med, 2012; 7: 52–53
13. Xu WH, Han YY, Wang SY, Ren MS: [Experimental rat models of experimental myasthenia gravis induced by Lewis, a murine acetylcholine receptor subunit 97–116.] Chinese Journal of Neuropsychiatric Diseases, 2006; 32: 179–80 [in Chinese]
14. Lennon VA, Lindstrom JM, Seybold ME: Experimental autoimmune myasthenia: A model of myasthenia gravis in rats and guinea pigs. J Exp Med, 1975; 141(6): 1365–75
15. Kent WJ, Sugnet CW, Furey TS et al: The human genome browser at UCSC. Genome Res, 2002; 12(6): 996–1006
16. Zhou Y, Zhou B, Pache L et al: Metascape provides a biologist-oriented resource for the analysis of systems-level datasets. Nat Commun, 2019: 10(1): 1523
17. Szklarczyk D, Gable AL, Lyon D et al: STRING v11: Protein-protein association networks with increased coverage, supporting functional discovery in genome-wide experimental datasets. Nucleic Acids Res, 2019; 47(D1): D607–13
18. Nel M, Prince S, Heckmann JM: Profiling of patient-specific myocytes identifies altered gene expression in the ophthalmoplegic subphenotype of myasthenia gravis. Orphanet J Rare Dis, 2019; 14(1): 24
19. Song J, Xi JY, Yu WB et al: Inhibition of ROCK activity regulates the balance of Th1, Th17 and Treg cells in myasthenia gravis. Clin Immunol, 2019; 203: 142–53
20. Wang S, Li H, Zhang M et al: Curcumin ameliorates experimental autoimmune myasthenia gravis by diverse immune cells. Neurosci Lett, 2016; 626: 25–34
21. Losen M, Martinez-Martinez P, Molenaar PC et al: Standardization of the experimental autoimmune myasthenia gravis (EAMG) model by immunization of rats with Torpedo californica acetylcholine receptors – Recommendations for methods and experimental designs. Exp Neurol, 2015; 270: 18–28
22. Mu L, Sun B, Kong Q et al: Disequilibrium of T helper type 1, 2 and 17 cells and regulatory T cells during the development of experimental autoimmune myasthenia gravis. Immunology, 2010; 128(1): e826–36
23. Ma CG, Zhang GX, Xiao BG, Link H: Cellular mRNA expression of interferon-gamma (IFN-γ), IL-4 and transforming growth factor-beta (TGF-β) in rats nasally tolerized against experimental autoimmune myasthenia gravis (EAMG). Clin Exp Immunol, 2010; 104(3): 509–16
24. Wang Y, Kunit T, Ciotkowska A et al: Inhibition of prostate smooth muscle contraction and prostate stromal cell growth by the inhibitors of Rac, NSC23766 and EHT1864. Br J Pharmacol, 2015; 172(11): 2905–291
25. Zhang X, Fang J, Chen S et al: Nonconserved miR-608 suppresses prostate cancer progression through RAC2/PAK4/LIMK1 and BCL2L1/caspase-3 pathways by targeting the 3'-UTRs of RAC2/BCL2L1 and the coding region of PAK4. Cancer Med, 2019: 8(12): 5716–34
26. Morrison AR, Yarovinsky TO, Young BD et al: Chemokine-coupled β2 integrin-induced macrophage Rac2-Myosin IIA interaction regulates VEGF-A mRNA stability and arteriogenesis. J Exp Med, 2014; 211(10): 1957–68
27. Ceneri N, Zhao L, Young BD et al: Rac2 modulates atherosclerotic Calcification by regulating macrophage interleukin-1β production. Arterioscler Thromb Vasc Biol, 2017; 37(2): 328–40
28. Yan Z, Ji-Bin X, Ke M et al: Rac2 deficiency attenuates CCl4-induced liver injury through suppressing inflammation and oxidative stress. Biomed Pharmacother, 2017; 94: 140–49
29. Bruder-Nascimento T, Callera GE, Montezano AC et al: Atorvastatin inhibits pro-inflammatory actions of aldosterone in vascular smooth muscle cells by reducing oxidative stress. Life Sci, 2019; 221: 29–34
30. Liu Y, Cheng G, Song Z et al: RAC2 acts as a prognostic biomarker and promotes the progression of clear cell renal cell carcinoma. Int J Oncol, 2019; 55(3): 645–56
31. Xia P, Gao X, Shao L et al: Down-regulation of RAC2 by small interfering RNA restrains the progression of osteosarcoma by suppressing the Wnt signaling pathway. Int J Biol Macromol, 2019; 137: 1221–31
32. Zhang X, Fang J, Chen S et al: Nonconserved miR-608 suppresses prostate cancer progression through RAC2/PAK4/LIMK1 and BCL2L1/caspase-3 pathways by targeting the 3'-UTRs of RAC2/BCL2L1 and the coding region of PAK4. Cancer Med, 2019; 8(12): 5716–34

Indexed in: [Current Contents/Clinical Medicine] [SCI Expanded] [ISI Alerting System] [ISI Journals Master List] [Index Medicus/MEDLINE] [EMBASE/Excerpta Medica] [Chemical Abstracts/CAS]

33. Parvaneh N, Mamishi S, Rezaei A et al: Characterization of 11 new cases of leukocyte adhesion deficiency type 1 with seven novel mutations in the ITGB2 gene. J Clin Immunol, 2010; 30(5): 756–60
34. Zhang Y, Li F, Wang H et al: Immune/inflammatory response and hypocontractility of rabbit colonic smooth muscle after TNBS-induced colitis. Dig Dis Sci, 2016; 61(7): 1925–40
35. Dai J, Xu LJ, Han GD et al: Down-regulation of long non-coding RNA ITGB2-AS1 inhibits osteosarcoma proliferation and metastasis by repressing Wnt/β-catenin signalling and predicts favourable prognosis. Artif Cells Nanomed Biotechnol, 2018; 46: S783–90
36. Liu M, Gou L, Xia J et al: LncRNA ITGB2-AS1 could promote the migration and invasion of breast cancer cells through Uu-regulating ITGB2. Int J Mol Sci, 2018; 19(7): pii: E1866
37. Lewis JB, Scangarello FA, Murphy JM et al: ADAP is an upstream regulator that precedes SLP-76 at sites of TCR engagement and stabilizes signaling microclusters. J Cell Sci, 2018; 131(21): pii: jcs215517
38. Li Y, Min W, Li M, et al. Identification of hub genes and regulatory factors of glioblastoma multiforme subgroups by RNA-seq data analysis. Int J Mol Med. 2016;38(4): 1170-1178.
39. Siggs OM, Miosge LA, Daley SR et al: Quantitative reduction of the TCR adapter protein SLP-76 unbalances immunity and immune regulation. J Immunol, 2015; 194(6): 2587–95
40. Bodié K, Buck WR, Pieh J et al: Biomarker evaluation of skeletal muscle toxicity following clofibrate administration in rats. Exp Toxicol Pathol, 2016; 68(5): 289–99
41. Maliver P, Festag M, Bennecke M et al: Assessment of preclinical liver and skeletal muscle biomarkers following clofibrate administration in Wistar rats. Toxicol Pathol, 2017; 45(4): 506–25
42. Sheng JJ, Jin JP: TNNI1, TNNI2 and TNNI3: Evolution, regulation, and protein structure – function relationships. Gene, 2016; 576(1): 385–94
43. Shu J, Ji G, Zhang M et al: Molecular cloning, characterization, and temporal expression profile of Troponin I type 1 (TNNI1) gene in skeletal muscle during early development of Gaoyou duck (*Anas platyrhynchos domestica*). Anim Biotechnol, 2019; 30(2): 118–28
44. De Matteis A, dell'Aquila M, Maiese A et al: The Troponin-I fast skeletal muscle is reliable marker for the determination of vitality in the suicide hanging. Forensic Sci Int, 2019; 301: 284–88
45. Cordiglieri C, Marolda R, Franzi S et al: Innate immunity in myasthenia gravis thymus: Pathogenic effects of Toll-like receptor 4 signaling on autoimmunity. J Autoimmun, 2014; 52: 74–89
46. Ji D, Zhou Y, Li S et al: Anti-nociceptive effect of dexmedetomidine in a rat model of monoarthritis via suppression of the TLR4/NF-κB p65 pathway. Exp Ther Med, 2017; 14(5): 4910–18

Indexed in: [Current Contents/Clinical Medicine] [SCI Expanded] [ISI Alerting System] [ISI Journals Master List] [Index Medicus/MEDLINE] [EMBASE/Excerpta Medica] [Chemical Abstracts/CAS]